Explicit Representation of Anisotropic Force Constants for Simulating Intermolecular Vibrations of Multiply Hydrogen-Bonded Systems

Hirohiko Houjou* and Ryota Koga†

Institute of Industrial Science, University of Tokyo, 4-6-1 Komaba, Meguro-ku, Tokyo 153-8505, Japan

Received: July 1, 2008; Revised Manuscript Received: August 17, 2008

We investigated the mechanical nature of multiply hydrogen-bonded systems by means of ab initio quantum chemical calculations, and we derived a set of force constants to reproduce the anisotropic vibration modes of such systems. Twenty multiply hydrogen-bonded molecular dimers were selected for evaluation of the stiffness of their hydrogen bonds. By means of a multivariate analysis, the principal values of the stiffness tensor were divided into the contributions from each hydrogen bond. Force constants in the stretching directions were estimated to be 20.2 and 11.5 N m^{-1} for NH···O and NH···N pairs, respectively. The obtained parameter set was used to reconstruct the various intermolecular vibration motions, and reasonable values in the low-frequency (ca. terahertz) region were obtained. Comparison of the multivariate analysis with the normal-mode analysis suggested that the off-diagonal terms for the transverse and rotational motions may appreciably contribute to the coupling of those basic motions.

1. Introduction

Systems of multiple hydrogen bonds serve as reversible and flexible cross-links in supramolecular polymers and supramolecular elastomers as well as in highly organized biomolecular structures such as proteins and nucleic acids.[1,2] The reversibility and moderate strength of hydrogen-bonded cross-links in these structures are responsible for such characteristic properties as thermal plasticity, viscoelasticity, and the dielectric property.[3] Introduction of a network of hydrogen bonds provides supramolecular polymers with practical properties, for example, mechanical strength, thermal durability, and non-Newtonian fluidity.[4−7]

Molecular building blocks that have the potential to form multiple hydrogen bonds are known as supramolecular synthons.[8] The greater the number of hydrogen bonds a synthon can form, the stronger it will be as a linker. Note that the term "strong" has two aspects, namely, stability and stiffness. From the viewpoint of energetic stability, the pioneering work of Jorgensen[9] clearly demonstrated that additivity and secondary interactions between the bonding pairs are important, although some cases that preclude the additivity rule have been reported.[10−13] In view of elasticity and dielectric response, such mechanical parameters as the restoring force provide more useful information than what energetic parameters do. For example, force constant parameters have been used to generate sets of normal-mode vibrational frequencies by means of analyses based on the Hessian matrix method, lattice dynamics, and Wiener−Khintchine's theorem combined with molecular dynamics calculations.[14−16] Comparison of theoretical and experimental vibrational spectra can provide a molecular-level picture of macroscopic phenomena of materials. Thus far, however, the mechanical properties of multiply hydrogen-bonded systems have not been as thoroughly studied as the energetic properties, especially in terms of additivity and secondary interactions between the individual hydrogen bonds.

Recently, terahertz spectroscopy has been used for direct observation of hydrogen bonding in the context of analyses of the hydration of sugars, the arrangement of nucleobases in DNA, the polymorphism of medicinal drugs, and so on.[17−19] The terahertz region (∼300 GHz to 3 THz) covers hydrogen bond vibrations, van der Waals interactions, overall molecular distortion, and molecular rotation, and hence, peak assignment is rather difficult. Accordingly, the theoretical simulation of spectra has been studied, and several quantum-chemical- and molecular-mechanics-based approaches have been reported.[20−26] The normal modes of multiple hydrogen bonds involve in-plane and out-of-plane vibrations, and distinguishing between the two implicitly requires that the force field parameters have anisotropic character. Although some parameter sets account for the anisotropy of the hydrogen bond,[27] reliable prediction of terahertz spectra requires the development of a "purpose-built" parameter set. In addition, as is often pointed out, the framework of the harmonic oscillator approximation may lead to serious deviation from experimental results.[28] It should be noted that vibrational anharmonicity of terahertz modes can also play a significant role in determining frequency shifts as well as absorption intensities. Now, at the primary stage of our study, it seems important to clarify the behavior of a hydrogen-bonded system around its potential minimum and hence to understand the fundamentals of spectra in the terahertz region. In this study, we investigated the mechanical nature of multiply hydrogen-bonded systems by means of ab initio quantum chemical calculations, and we derived a set of force constants to reproduce the anisotropic vibration modes of such systems.

2. Theoretical Basis

2.1. Formulation of Anisotropic Force Constants. If functional groups −XH and Y− exert a hydrogen-bonding force $\mathbf{F}_{HB}$ on each other originating in the hydrogen-bonding potential $\phi(\mathbf{r})$, the force vector should be divided into three anisotropic components of an appropriately selected coordinate system according to the molecular symmetry. At the potential minimum, atom X is located at the origin, atom H is on the x axis, and the hydrogen bond acceptor (Y) is located at (x, y, z). Upon first-

* To whom correspondence should be addressed. Phone: +81(3)5452-6367. Fax: +81(3)5452-6366. E-mail: houjou@iis.u-tokyo.ac.jp.
† Present affiliation: X-Ability Co., Ltd.

10.1021/jp8057614 CCC: $40.75
Published on Web 10/04/2008

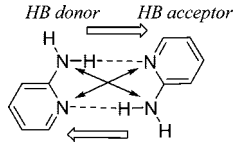

Figure 1. Secondary interactions of hydrogen bond donors and acceptors. In this 2-aminopyridine dimer, there are two antiparallel NH···N bonds; hence, $q = 2$ (the number of double-headed arrows).

order expansion of $\mathbf{F}_{HB}$ around the potential minimum (x_0, y_0, z_0), a force constant matrix $\mathbf{K}$ can be defined as follows:

$$\mathbf{F}_{HB} = -\nabla \cdot \phi(r) = -\begin{pmatrix} k_{11} & k_{12} & k_{13} \\ k_{21} & k_{22} & k_{23} \\ k_{31} & k_{32} & k_{33} \end{pmatrix}\begin{pmatrix} x - x_0 \\ y - y_0 \\ z - z_0 \end{pmatrix} \quad (1)$$

where

$$k_{ij} = \frac{d^2\phi}{dx_i\, dx_j}^{x_i = x_{i0}, x_j = x_{j0}}$$

When $\phi(\mathbf{r})$ is an isotropic function such as a Lennard-Jones-type potential, $\phi(r)$ is a function of a unique argument r, the norm of $\mathbf{r}$. Then each component k_{ij} can be written as

$$k_{ij} = \begin{cases} \dfrac{d^2\phi}{dr^2}\dfrac{x_{i0}^2}{r^2} + \dfrac{d\phi}{dr}\dfrac{r^2 - x_{i0}^2}{r^3} \; (i = j) \\ \dfrac{d^2\phi}{dr^2}\dfrac{x_{i0}x_{j0}}{r^2} - \dfrac{d\phi}{dr}\dfrac{x_{i0}x_{j0}}{r^3} \; (i \neq j) \end{cases} \quad (2)$$

Some of these terms vanish depending on the nature of $\phi(r)$. For example, if one assumes that the XH···Y pair acts as a harmonic oscillator, then $\phi(r)$ is a quadratic function, $\phi(r) = a(r - r_0)^2 + b$, where r_0 is the distance between X and Y at equilibrium. When Y is at position (r_0, 0, 0), the force constants k_{ij} are given by

$$k_{11} = 2a \;\; k_{22} = k_{33} = 0 \; k_{12} = k_{21} = k_{13} = k_{31} = k_{23} = k_{32} = 0 \quad (3)$$

The first term of k_{ii} ($i = 2, 3$) vanishes owing to the isotropic character of $\phi(r)$, and the second term vanishes owing to the harmonic approximation. The off-diagonal terms k_{ij} can be eliminated by selecting the coordination system to fit the molecular symmetry. Therefore, if k_{22} and k_{33} are explicitly evaluated, then either the anisotropy or the nonharmonic character of the hydrogen-bonding potential, or both, must be incorporated.[29]

When we applied the above potential for a single hydrogen bond to multiply hydrogen-bonded systems, we assumed that the force exerted between a pair of molecules can be divided into the contribution of each individual hydrogen bond and the contributions of secondary interactions between neighboring hydrogen bond donors and acceptors (Figure 1). The force constants of NH···N and NH···O pairs were designated k_{NH-N} and k_{NH-O}, respectively (OH···O and OH···N pairs were not studied in this work). The idea of introducing the secondary interactions was inspired by the work of Jorgensen, who attempted to interpret energetic stability by considering the arrangement of donor−acceptor (XH···Y) pairs.[9] We took into account two different types of force constants: one (k_{para}) for the parallel arrangement of XH···Y pairs and one (k_{anti}) for antiparallel arrangement. For simplicity, differences in the hybridization states of the atoms were neglected; for example, amino NH and amide NH were treated identically. Consequently, the intermolecular force $\mathbf{F}_i$ induced by ith direction displacement is given by

$$\mathbf{F}_i = -\{m(k_{NH-O})_{ii} + n(k_{NH-N})_{ii} + p(k_{para})_{ii} + q(k_{anti})_{ii}\} \times (x_i - x_{i0}) \equiv -K_i(x_i - x_{i0}) \quad (4)$$

Coefficients m and n are the numbers of NH···O and NH···N hydrogen bonds, respectively, in the dimeric system in question. Coefficients p and q are the number of diagonally opposite donor−acceptor pairs and that of either acceptor−acceptor or donor−donor pairs, respectively. These parameters serve as cross-terms, whether or not the donors and acceptors are actually involved in a hydrogen bond. In the 2-aminopyridine dimer (Figure 1), for example, two NH···N bonds are aligned in antiparallel form, so $m = 0$, $n = 2$, $p = 0$, and $q = 2$. The components of the force constants, k_{NH-O} and k_{NH-N}, represent the contributions of NH···O and NH···N hydrogen bonds, respectively, and k_{para} and k_{anti} represent neighboring interactions of hydrogen bonds in parallel and antiparallel alignments, respectively.

Accordingly, $\mathbf{F}_{HB}$ can be formulated as a function of the shear vector:

$$\mathbf{F}_{HB} = -\begin{pmatrix} K_1 & 0 & 0 \\ 0 & K_2 & 0 \\ 0 & 0 & K_3 \end{pmatrix}\begin{pmatrix} x - x_0 \\ y - y_0 \\ z - z_0 \end{pmatrix} \quad (5)$$

According to the above formulation, the hydrogen-bonding energy is derived as follows:

$$E_{HB} = \frac{1}{2}\{K_1(x - x_0)^2 + K_2(y - y_0)^2 + K_3(z - z_0)^2\} - E_{HB}^{(0)} \quad (6)$$

where $E_{HB}^{(0)}$ is the hydrogen-bonding energy at the potential minimum. Alternatively, E_{HB} can be defined as the association energy E_{assoc} that is obtained by subtracting the total energy of the constituting monomers from that of the dimer:

$$E_{HB} = E_{assoc} = E_{dimer} - E_{monomer\,1} - E_{monomer\,2} \quad (7)$$

Therefore, once the association energy was obtained as a function of the displacement vector, the force constants K_i were calculated by regression analysis based on quadratic functions of x_i.

2.2. Calculations. Twenty hydrogen-bonded dimers (**1**−**20**; Figure 2) were studied. The geometry of each dimer was optimized by means of the Hartree−Fock (HF) method using the 6-311G** basis set. Then the association energy E_{assoc} was calculated at the same level either with or without correction for the basis set superpositional error (BSSE) by means of the counterpoise method, and the energy was also calculated by the MP2 perturbation method using the same basis set. The potential curve of the association was obtained by scanning the center of mass of each monomer in 0.05 Å increments in the x, y, and z directions. In every step of the scan, all the geometrical parameters were fixed (i.e., the frozen rigid approximation was used), and the alignment of the coordination system of each monomer was retained. The frozen rigid approximation is appropriate for this study because our purpose was to reproduce terahertz region vibrations that are essentially whole-molecule motion. All calculations were performed using the Gaussian03w program.[30]

Basically, the local minimum structure was confirmed by the normal-mode vibrational analysis. When we had difficulty in optimizing the structure, some of the geometrical parameters were fixed so as not to influence the evaluation of the hydrogen-bonding strength. For structures **1**−**3**, for example, the amide

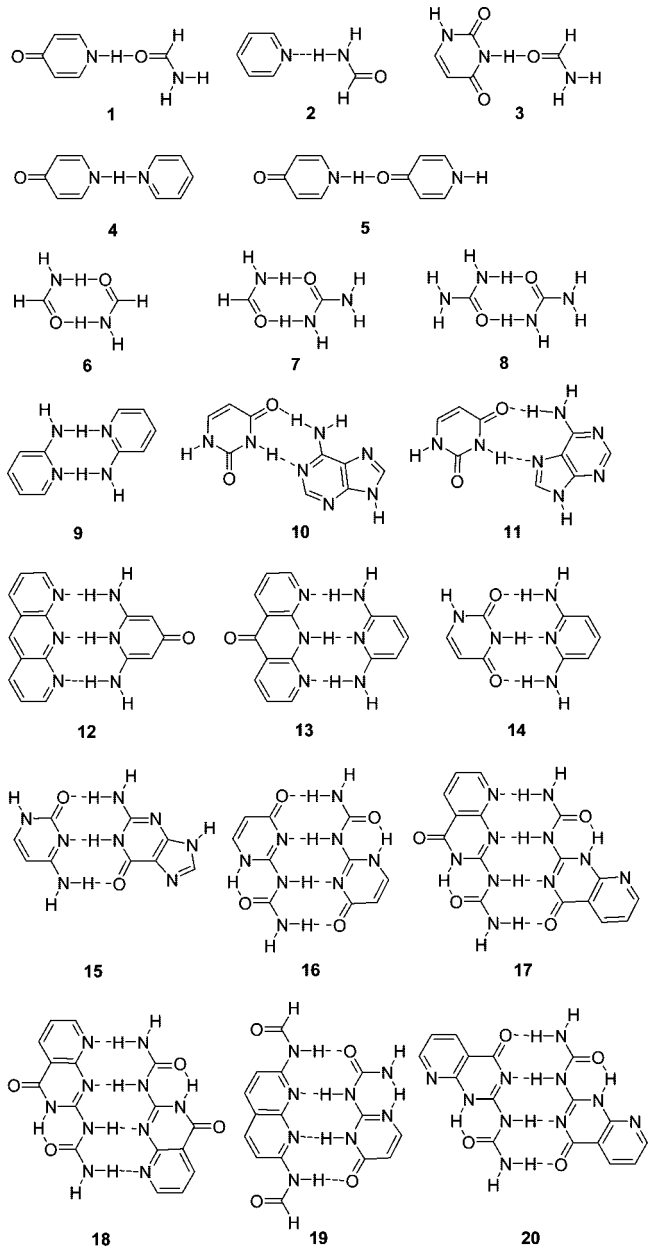

Figure 2. Chemical structures of the molecular dimers studied.

plane was forced perpendicular to the heterocyclic plane, with the hydrogen bond running along the x axis. For the other cases, the coordination system was set up so that the molecular planes fell on the xy plane, with the hydrogen bond running along the x axis. In molecules in which the amino group(s) was found to be in a pyramidal form, the structure was fixed to a planar form (saddle point structure) to avoid ambiguity in the selection of the displacement direction. This treatment is appropriate because the activation energy of the flip-flop conversion between the pyramidal forms of the amino group is much less ($<\sim$10%) than the error in the subsequent regression analysis.

3. Results and Discussion

3.1. Derivation of Force Constants. Figure 3 shows potential curves for the 2-aminopyridine dimer obtained when the dimer's center of mass was scanned along the x axis (for the coordinates used, see the "Calculations" section). Similar results were obtained for the scans along the y and z axes. The curves are well fitted by quadratic functions in the range from -0.25 to $+0.25$ Å around the potential minimum. This range agrees fairly well with the amplitude of interatomic oscillation in the classical picture of the vibrational spectrum. From regression analysis of the potential curves, force constants K_1, K_2, and K_3 were derived at the HF and MP2 levels (Table 1).

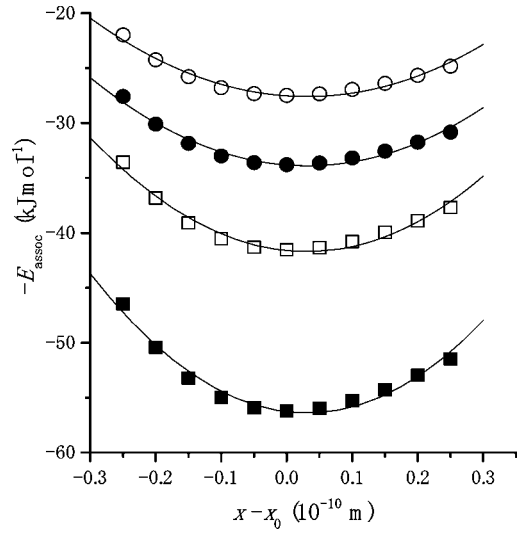

Figure 3. Potential curve for stretching of the 2-aminopyridine dimer in the x direction: HF (●), HF + BSSE correction (○), MP2 (■), MP2 + BSSE correction (□). The solid lines are the least-squares fitting against the quadratic function.

TABLE 1: Force Constants Derived by Regression Analysis of Data from HF and MP2 Calculations Either with or without BSSE Correction

	force constants K (N m^{-1})			
	K_1	K_2	K_3	$E_{HB}^{(0)}$ (kJ mol^{-1})
HF/6-311G**//HF/6-311G**	24.34	9.25	3.90	33.79
HF/6-311G**//HF/6-311G** + BSSE correction	21.71	8.44	3.84	27.49
MP2/6-311G**//HF/6-311G**	38.49	12.35	5.59	56.21
MP2/6-311G**//HF/6-311G** + BSSE correction	31.50	10.22	5.73	41.56

Although the K values depended on the calculation level, the trend of the change in K is quite understandable. Because the basis set overlap underestimated the total energy when two monomers were close to each other, the correction by the counterpoise method resulted in a decrease in the K values. This decrease in K was prominent for K_1 (displacement in the x direction). The incorporation of electronic correlation energy by means of the MP2 method resulted in a decrease in the total energy, especially around the potential minimum, which led to an increase in the K values. Therefore, these two corrections are expected to compensate for each other. Indeed, when both corrections, i.e., electronic correlation and counterpoise, were taken into account, the K values fell between those obtained by means of either correction alone. For the sake of saving time, we thus carried out the calculations at the HF/6-311G**//HF/6-311G** level, and these calculations gave reasonable K values in view of the cancellation of the two corrections. This calculation might give an error of $\sim$20%, but the relative amplitude of the displacement directions and the types of hydrogen bonds are expected to be retained.

Table 2 summarizes the regression coefficients for **1**−**20** derived from eq 6. Table 2 also contains the parameters m, n, p, and q, which were determined from the hydrogen-bonding pattern of the dimers (see the "Theoretical Basis" section). The

TABLE 2: Regression Coefficients of Dimeric Structures

					force constants K (N m^{-1})			
dimer	m	n	p	q	K_1	K_2	K_3	$E_{HB}^{(0)}$ (kJ mol^{-1})
Single HB								
1	1	0	0	0	20.37	0.72	0.33	34.97
2	0	1	0	0	14.53	4.35	2.70	25.05
3	1	0	0	2	17.90	2.65	0.68	19.51
4	0	1	0	0	18.92	5.67	1.90	33.49
5	1	0	0	0	24.43	0.97	0.73	43.8
Double HB								
6	2	0	0	2	35.08	8.00	6.86	52.98
7	2	0	0	2	36.96	8.65	7.10	48.56
8	2	0	0	2	38.64	9.22	6.68	54.65
9	0	2	0	2	24.34	9.25	3.90	33.79
10	1	1	0	3	35.98	12.47	5.08	47.27
11	1	1	0	3	36.81	12.04	4.91	49.50
Triple HB								
12	0	3	4	0	33.27	3.32	6.34	59.67
13	0	3	0	4	31.77	14.38	1.08	33.18
14	2	1	0	4	41.99	15.41	5.15	51.89
15	2	1	2	2	60.08	11.87	8.12	100.79
Quadruple HB								
16	2	2	4	2	88.89	12.96	13.04	161.24
17	1	3	4	2	74.89	12.74	11.56	118.98
18	0	4	4	2	66.36	12.94	11.16	113.94
19	2	2	2	4	75.37	18.01	8.56	132.42
20	2	2	4	2	83.04	12.58	13.04	124.97

values of the coefficients in the table roughly depended on the structure of the dimer: as the multiplicity of hydrogen bonding increased, both K and E_{HB} increased, indicating that these values were composed of the contributions from the individual hydrogen bonds. However, it is also obvious that simple additivity does not hold.

To abstract a simple relationship for these data, we utilized multivariate analysis.[31] Namely, we determined the values of k_{NH-O}, k_{NH-N}, k_{para}, and k_{anti} so that the K value could be best reproduced as a function of m, n, p, and q based on eq 4 by a least-squares method. Figure 4 shows the correlation between the K values directly obtained from the quadratic curve fitting and the values (K') obtained from the multivariate analysis. As can be seen from this figure, K and K' are in good agreement ($r = 0.92-0.96$). Although the data/variable ratio ($20/4 = 5$) was not high, the good correlation suggests that the proposed model (eq 5) is acceptable. The present model may be too simplified, but it would not be expedient to use additional parameters that lower the data/variable ratio. Table 3 summarizes the values of each contribution to the force constant K.

The k_{NH-O} and k_{NH-N} values represent the anisotropy of the restoration forces of NH···O and NH···N interactions, respectively. Although the x component, which represents stretching elasticity, predominated, the y and z components (bending elasticity) made appreciable contributions (10−30% of the x component contribution). These contributions are large enough to infer that the force field is intrinsically anisotropic.[29] The x components of the k_{NH-O} and k_{NH-N} values are as reasonable as the force constants (10−20 N m^{-1}) of normal hydrogen bond stretching. Interestingly, the results imply that the NH···O bond has uniaxial symmetry, whereas the NH···N bond has biaxial symmetry. Although we need further detailed analysis, we can assume that this difference arose from the anisotropy of the electronic distribution in acceptor atom Y. For a carbonyl oxygen atom, the 2s, $2p_z$, and $2p_y$ orbitals contribute equally to the electronic distribution around the x axis; hence, the tolerance for bending of the hydrogen bond in the y direction is equal to that for bending in the z direction. In contrast, because the $2p_y$ orbital is fully concerned in the σ bond of the imino nitrogen

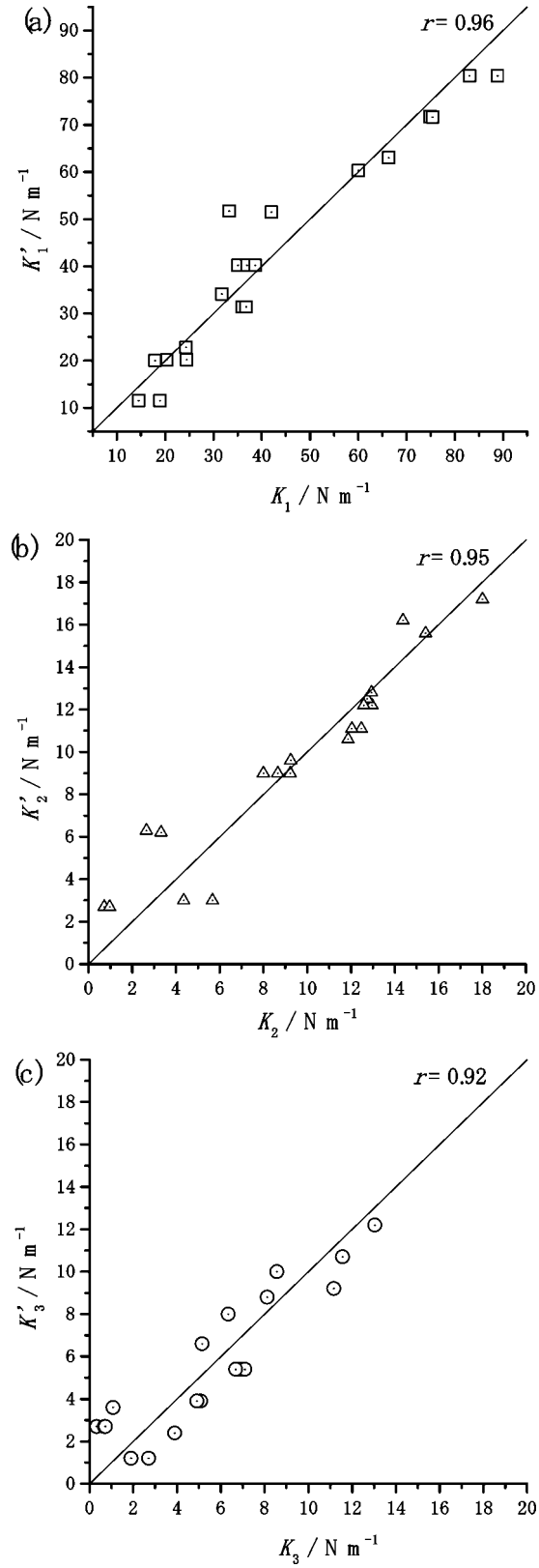

Figure 4. Correlation of the principal values of stiffness tensors derived from ab initio calculations (K_i) and those reconstructed from the contributions listed in Table 3 (K_i').

TABLE 3: List of Contributions k (N m^{-1}) to Force Constants K_i ($i = x, y, z$)

axis	k_{NH-O}	k_{NH-N}	k_{para}	k_{anti}
x	20.2	11.5	4.3	−0.1
y	2.7	3.0	−0.7	1.8
z	2.7	1.2	1.1	0

atom, the electronic distribution is rather localized in the xz plane, resulting in a smaller tolerance (larger k value) for shear in the y direction.

The k_{para} and k_{anti} values represent the effects of neighboring hydrogen bond donor−acceptor interactions. The relatively large contribution of k_{para} (4.3 N m^{-1}) to K_1 (the x component) can be interpreted in terms of Coulombic attraction, and the negligible contribution of k_{anti} (−0.1 N m^{-1}) suggests that attractive and repulsive Coulombic interactions are canceled in the antiparallel alignment. A similar interpretation is valid for the z components of k_{para} and k_{anti} (1.1 and 0 N m^{-1}, respectively). The contributions of k_{para} and k_{anti} (−0.7 and 1.8 N m^{-1}, respectively) to K_2 (the y component) are rather small but not negligible, and they oppose each other. This relationship can also be explained in terms of electrostatic interactions. For example, for two hydrogen bonds in a parallel arrangement (Figure 5a), displacement in the y direction leads to attractive interactions, which decrease the curvature of the potential surface. Therefore, the parallel arrangement gives a negative contribution to K_2. In contrast, for two hydrogen bonds in an antiparallel arrangement (Figure 5b), displacement in the y direction leads to repulsive interactions, which increase the curvature. Therefore, the antiparallel arrangement gives a positive contribution to K_2.

3.2. Validation of the Force Constants. In the above section, we discussed how the contributions (k_{NH-O}, k_{NH-N}, k_{para}, and k_{anti}) to each component of the K value were obtained, and we clarified their physical meaning. Although the k values may depend on the calculation method and on the structures used for multivariate analysis, the expected maximum error is ∼20%. These parameters should be validated by comparison with various experimental results and should be consistent with parameters obtained by means of other theoretical methods. For example, normal-mode analysis is a powerful method for interpreting experimental absorption peaks. For the stretching vibration of hydrogen-bonded pairs, there have been some attempts to derive force constants on the basis of the comparison of experimental and theoretical analyses of normal-mode vibrations.[32] These studies suggest that the stretching force constants are in the range of 10−20 N m^{-1}, and our results agree fairly well with this range. Figure 6 illustrates the normal-mode vibrations for a dimer that originate mainly in distortion of the hydrogen-bonding system.[33] Out of the six modes shown, only two (stretch and opening) can be explained by assigning the x component of the force constants to each bond; the other four modes (shear, propeller twist, buckle, and stagger) require y and z components. Therefore, our results given in Table 3 play a decisive role in evaluating the frequencies of these intermolecular vibrational modes in the framework of molecular mechanics approximation.

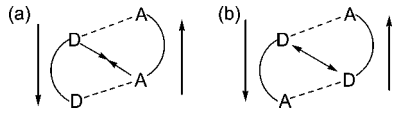

Figure 5. Neighboring interactions in a y-sheared dimer.

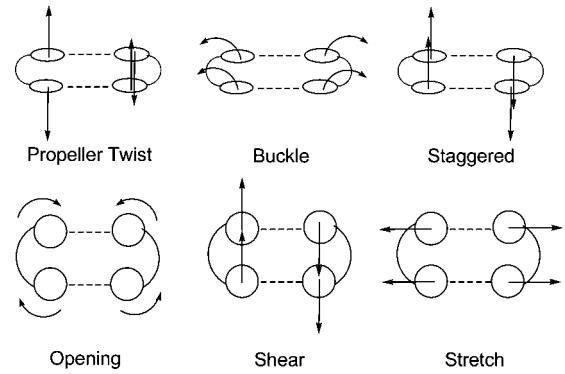

Figure 6. Representative intermolecular vibration modes.

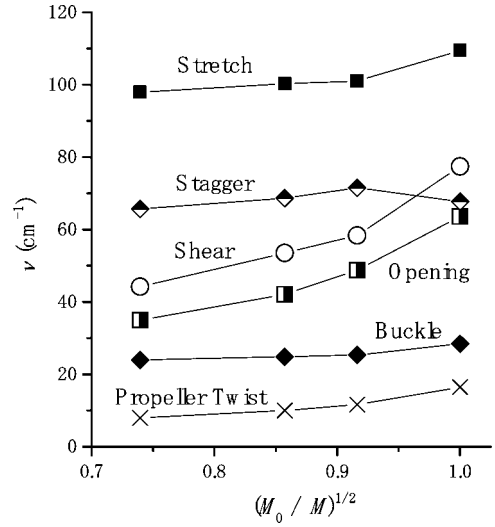

Figure 7. Frequencies of intermolecular vibration modes of 5-substituted 2-aminopyridines as a function of the square root of the relative molecular weight $(M_0/M)^{1/2}$.

Leutwyler et al. estimated the force constant of NH···O stretching in a 2-pyridone homodimer to be 37.7 N m^{-1} on the basis of a two-color resonant two-photon ionization (2C-R2PI) spectroscopy measurement.[34a,b] They also report that the stretching force constant of the 2-hydroxypyridine−2-pyridone heterodimer is 70 N m^{-1} (35 N m^{-1} per hydrogen bond).[34d] These values are very large as compared to the normal range, and the authors suggest the effects of resonance-assisted hydrogen bonding.[13] On the other hand, by assuming that the force constant of 35 N m^{-1} is assigned to NH···N stretching, the force constant of NH···O in the 2-aminopyridine−2-pyridone heterodimer was estimated to be 17 N m^{-1}.[34c] Although this value is in good agreement with our k_{NH-O} value (20.2 N m^{-1}), the overall results contradict ours. In those studies, the force constants were derived by means of the pseudodiatomic approximation, in which each monomer is regarded as a point with a mass equal to its molecular weight.[32] In addition, the result was based on simple additivity of the force constants. To gain insight into the hydrogen bond vibrations and to clarify the limitation of the pseudodiatomic approximation, we performed normal-mode calculations on a series of 5-halogenated 2-aminopyridine dimers. Figure 7 shows the frequencies (ν, cm^{-1}) of the normal modes corresponding to those in Figure 6 as functions of the square root of M_0/M, where M is the molecular weight of a monomer and M_0 is the molecular weight of 2-aminopyridine. Ideally, the frequency should be proportional to $(M_0/M)^{1/2}$. As shown in Figure 7, the frequencies are approximately linearly related to $(M_0/M)^{1/2}$ for shear, opening,

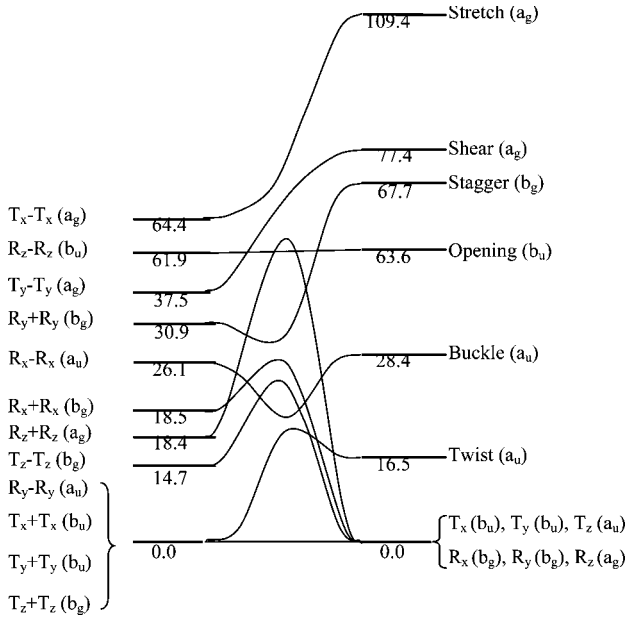

Figure 8. Correlation diagram of intermolecular vibration modes between the monomers (left) and dimers (right). The number below each level is the frequency (cm^{-1}).

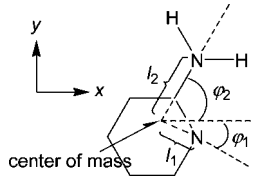

Figure 9. Geometrical parameters used for calculating the modal vibration of 2-aminopyridine.

and propeller twist, whereas the frequencies of the other four modes are relatively insensitive to M.

This observation suggests that the pseudodiatomic approximation does not always work appropriately. The frequency of the stretch mode tended to be higher than that expected from the molecular weight. This discrepancy must have arisen from the fact that the frequency of the intermolecular vibration depends on the moment of inertia around an axis through the center of mass of each molecule.[35] Consequently, one reason for the discrepancy between the force constants derived from the 2C-R2PI experiment and those derived from our own experiments is the treatment of the reduced mass of the molecules. However, it should also be noted that our present model is based on a frozen rigid approximation and therefore cannot account for any coupling terms between intermolecular vibration (whole-molecule motion) modes and intramolecular vibration (localized diatomic motion, for example) modes. If a molecular system is subject to resonance-assisted hydrogen-bonding effects,[13] the frozen rigid approximation would result in appreciable errors.

Here we qualitatively explain the dependence of the frequency on the molecular weight. If we assume that a molecular dimer has C_{2h} symmetry, we can assign an irreducible representation to each normal mode as follows: propeller twist (a_u), buckle (a_u), opening (b_u), shear (a_g), stagger (b_g), and stretch (a_g). As can be seen from Figure 6, each normal mode is a combination of the transverse (T_x, T_y, and T_z) and rotational (R_x, R_y, and R_z) motions of each monomer unit. Therefore, the displacement vectors of these motions can be described in a 12-dimensional space that is expanded by the displacement vectors of the T_x, T_y, T_z, R_x, R_y, and R_z motions. Here the notation $T_x + T_x$, for example, refers to a symmetric combination of T_x. In view of the symmetry of these basic motions, the shear and stretch modes are composed of the combinations $T_x - T_x$, $T_y - T_y$, and $R_z + R_z$, all of which are assigned to an a_g representation. For all the modes, the correlation between the normal modes and the basic motions is schematically illustrated in Figure 8. The apparent insensitivity of the frequency to the molecular weight (Figure 7) may have arisen from the complicated mixing of basic transverse and rotational motions, as shown in Figure 8.

Of the six intermolecular vibration modes, only opening has a b_u representation, originating in $R_z - R_z$ motion. This finding explains the fact that the frequency of the opening mode is approximately proportional to $(M_0/M)^{1/2}$. Because the $R_z - R_z$ vibration originates from an antisymmetric stretching of the NH···N bond, the stretch elasticity of this bond is more directly reflected in the opening mode than in the stretch mode. Using the force constants derived above, we attempted to calculate the frequency of $R_z + R_z$ and $R_z - R_z$ mode vibrations by purely mechanical means. Using the geometrical parameters shown in Figure 9, one can obtain eigenvalues, $I_z\omega^2$, of the equation of motion:

$$R_z - R_z \text{ mode: } I_z\omega^2 = K_1 + K_2 \quad (8a)$$

$$R_z + R_z \text{ mode: } I_z\omega^2 = K_1 - K_2 \quad (8b)$$

K_1 and K_2 are defined as follows:

$$K_1 = k_x(l_1^2 \sin^2\phi_1 + l_2^2 \sin^2\phi_2) - k_y(l_1^2 \cos^2\phi_1 + l_2^2 \cos^2\phi_2) \quad (9a)$$

$$K_2 = 2k_x l_1 l_2 \sin\phi_1 \sin\phi_2 + 2k_y l_1 l_2 \cos\phi_1 \cos\phi_2 \quad (9b)$$

Because the 2-aminopyridine dimer is an antiparallel doubly hydrogen-bonded system, the force constants of the hydrogen bonds are $k_x = 11.5$ N m^{-1} and $k_y = 4.8$ N m^{-1}. The moment of inertia I_z around the z axis through the center of mass was calculated to be 4.44×10^{-45} kg m^2. Then we obtained 61.9 and 18.4 cm^{-1} as the frequencies ω of the $R_z - R_z$ and $R_z + R_z$ modes, respectively. The value of 61.9 cm^{-1} is in good agreement with the frequency (63.6 cm^{-1}) of the opening mode. This agreement confirms that our analysis based on mechanical parameters and the normal-mode analysis based on a rigorous Hessian matrix treatment give consistent results. We must emphasize that our strategy, namely, the segmentation of intermolecular force constants into the contributions from constituent hydrogen bonds, enabled us to correctly reproduce an intermolecular bending force from the force constants for transverse deformation. For the other 11 basic modes, similar calculations gave the corresponding frequencies of vibration (Figure 8), and all the calculated values were within a reasonable low-frequency range. The correspondence between the levels of the 12 basic motions and the 6 normal modes is not simple, suggesting that the off-diagonal terms such as $T_x - T_x$ versus $R_z + R_z$ appreciably contribute to the normal-mode frequencies. In addition, it should also be noted that the normal-mode analysis was performed for the energy minimum structure, which has not C_{2h} symmetry but C_i symmetry, because of the pyramidization of the amino group; this fact results in contamination of a_g with b_g representations and contamination of a_u with b_u representations. Implementation of the coupling effect of the vibrational modes into more-practical simulations, such as lattice dynamics, would require another approach, including a detailed analysis of the eigenvectors of normal-mode vibrations.

4. Conclusions

We formulated an explicit representation of anisotropic force constants to realistically describe the motion of interacting molecules. We applied the formulation to multiply hydrogen-bonded systems and demonstrated that the stiffness of a hydrogen bond has apparent anisotropy, responsible for the occurrence of several types of intermolecular vibration modes. On the basis of a multivariate analysis of 20 molecular dimer systems with one to four hydrogen bonds, we succeeded in dividing the force constants into the contributions of each hydrogen bond (NH···N or NH···O) and each secondary interaction with neighboring hydrogen-bonded pairs in a parallel or an antiparallel alignment. The principal values of the stiffness tensor were 20.2, 2.7, and 2.7 N m^{-1} for the NH···O bond and 11.5, 3.0, and 1.2 N m^{-1} for the NH···N bond. The results suggested that the symmetry of the tensors is related to the hybridization of the atoms in question. The secondary interactions were relatively small but not negligible, and the difference in parameters k_{para} and k_{anti} accounts for the difference in intermolecular forces between the systems with various alignments of the hydrogen bonds. The origin of the secondary interactions can be qualitatively explained in terms of electrostatic interactions. Although the stiffness tensor values had an intrinsic error of ∼20% that came from the precision of calculation, we expect that the relative magnitude of anisotropy and the additivity of the contributions are intrinsic properties of the hydrogen-bonded system, and hence, they are not much influenced by the level of calculation.

The consistency between our force constants and the experimental and theoretical normal-mode vibrational frequencies was also checked. The difference in force constants k_{NH-N} and k_{NH-O} between the 2C-R2PI results and ours may originate from an inappropriate derivation of force constants from experimental data or from a lack of the resonance-assisted effects in calculation. By means of a mechanical method, we derived the frequencies of 12 basic motions that are represented as a combination of transverse and rotational motions of the monomers. The good agreement between the observed and calculated frequency regions validated our approach in collecting the parameters, although the discrepancy between the frequency values highlighted the importance of off-diagonal terms of transverse versus rotational motions. We pointed out that the nature of the normal-mode vibrations must be considered in discussions of force constants based on spectral data. Classification of the normal mode based on group theory led us to the important deduction that the stretch elasticity was not purely reflected in the stretch mode, but was directly reflected in the opening mode. Our parameters reproduced fairly well the frequency of the opening mode derived from normal-mode analysis. Through the comparison between mechanical and quantum calculations, we demonstrated that the parameter set is valid for calculating the bending stiffness, even though the set was derived from transverse displacement only. We expect that these parameters will be effective for simulating various intermolecular motions in biological systems and condensed matter.

References and Notes

(1) *Supramolecular Polymers*, 2nd ed.; Ciferri, A., Ed.; Taylor & Francis: New York, 2005.

(2) (a) Hofmeier, H.; Schubert, U. S. *Chem. Commun.* **2005**, 2423–2432. (b) Sivakova, S.; Rowan, S. J. *Chem. Soc. Rev.* **2005**, *34*, 9–21. (c) Brunsveld, L.; Folmer, B. J.; Meijer, E. W.; Sijbesma, R. P. *Chem. Rev.* **2001**, *101*, 4071–4097.

(3) (a) Hilger, C.; Stadler, R.; Freitas, L. L. D. *Polymer* **1990**, *31*, 818–823. (b) Muller, M.; Seidel, U.; Stadler, R. *Polymer* **1995**, *36*, 3143–3150. (c) Muller, M.; Stadler, R.; Kramer, F.; Williams, G. R. *Macromolecules* **1995**, *28*, 6942–6949.

(4) Chino, K.; Ashiura, M. *Macromolecules* **2001**, *34*, 9201–9204.

(5) Peng, C. C.; Abetz, V. *Macromolecules* **2005**, *38*, 5575–5580.

(6) Zhao, Y. Q.; Beck, J. B.; Rowan, S. J.; Jamieson, A. M. *Macromolecules* **2004**, *37*, 3529–3531.

(7) Leibler, L.; Rubinstein, M.; Colby, R. H. *Macromolecules* **1991**, *24*, 4701–4707.

(8) Desiraju, G. R. *Angew. Chem., Int. Ed. Engl.* **1995**, *36*, 2311–2327.

(9) Jorgensen, W. L.; Pranata, J. *J. Am. Chem. Soc.* **1990**, *112*, 2008–2010.

(10) Popelier, P. L. A.; Joubert, L. *J. Am. Chem. Soc.* **2002**, *124*, 8725–8729.

(11) Liu, W. H.; Chen, G. J. *Phys. Chem. Chem. Phys.* **2005**, *7*, 3943–3947.

(12) Asensio, A.; Kobko, N.; Dannenberg, J. J. *J. Phys. Chem. A* **2003**, *107*, 6441–6443.

(13) Gilli, G.; Bellucci, F.; Ferretti, V.; Bertolasi, V. *J. Am. Chem. Soc.* **1989**, *111*, 1023–1028.

(14) Spirko, V.; Sponer, J.; Hobza, P. *J. Chem. Phys.* **1997**, *106*, 1472–1479.

(15) Willock, D. J.; Price, S. L.; Leslie, M.; Catlow, C. R. A. *J. Comput. Chem.* **1995**, *16*, 628–647.

(16) (a) Weiner, S. J.; Kollman, P. A.; Case, D. A.; Singh, U. C.; Ghio, C.; Alagona, G.; Profeta, S., Jr.; Weiner, P. *J. Am. Chem. Soc.* **1984**, *106*, 765. (b) Cornell, W. D.; Cieplak, P.; Bayly, C. I.; Gould, I. R.; Merz, K. M.; Ferguson, D. M.; Spellmeyer, D. C.; Fox, T.; Caldwell, J. W.; Kollman, P. A. *J. Am. Chem. Soc.* **1995**, *117*, 5179–5197.

(17) (a) Heyden, M.; Bründermann, E.; Heugen, U.; Niehues, G.; Leitner, D. M.; Havenith, M. *J. Am. Chem. Soc.* **2008**, *130*, 5773–5779.

(18) Fischer, B. M.; Walther, M.; Jepsen, P. U. *Phys. Med. Biol.* **2002**, *47*, 3807–3814.

(19) Taday, P. F.; Bradley, I. V.; Arnone, D. D.; Pepper, M. *J. Pharm. Sci.* **2003**, *92*, 831–838.

(20) Rungsawang, R.; Ueno, Y.; Tomita, I.; Ajito, K. *J. Phys. Chem. B* **2006**, *110*, 21259–21263.

(21) Takahashi, M.; Ishikawa, Y.; Nishizawa, J.; Ito, H. *Chem. Phys. Lett.* **2005**, *401*, 475–482.

(22) Day, G. M.; Zeitler, J. A.; Jones, W.; Rades, T.; Taday, P. F. *J. Phys. Chem. B* **2006**, *110*, 447–456.

(23) Siegrist, K.; Bucher, R.; Mandelbaum, I.; Walker, A. R. H.; Balu, R.; Gregurick, S. K.; Plusquellic, D. F. *J. Am. Chem. Soc.* **2006**, *128*, 5764–5775.

(24) Fedor, A. M.; Korter, T. M. *Chem. Phys. Lett.* **2006**, *429*, 405–409.

(25) Saito, S.; Inerbaev, T. M.; Mizuseki, H.; Igarashi, N.; Note, R.; Kawazoe, Y. *Chem. Phys. Lett.* **2006**, *423*, 439–444.

(26) Korter, T. M.; Balu, R.; Campbell, M. B.; Beard, M. C.; Gregurick, S. K.; Heilweil, E. J. *Chem. Phys. Lett.* **2006**, *418*, 65–70.

(27) Lii, J. H.; Allinger, N. L. *J. Comput. Chem.* **1998**, *19*, 1001–1016.

(28) Ma, J. *Structure* **2005**, *13*, 373–380.

(29) For an isotropic potential function, $\phi(r) = a(r - r_0)^2 + b$, the x component of the associative force **F** is expanded around $r_0 = (x_0, 0, 0)$ as follows: $\mathbf{F}_x = 2a\{(x - x_0) + y^2/2x_0 + z^2/2x_0\}$. Obviously, this formulation assumes the nonlinear restoration response along the y and z axes. The explicit evaluation of k_{22} and k_{33} in the framework of harmonic approximation corresponds to the replacement of $k_{22} = ay/x_0$ and $k_{33} = az/x_0$, respectively. The k_{22} and k_{33} values are estimated at most as 5% of $2a$ ($=k_{11}$) under the conditions used in this study ($x_0 \approx 3$ Å, $|y| = |z| \approx 0.3$ Å). Thus, the k_{22} and k_{33} values of more than 5% of k_{11} imply a genuine anisotropy of the force field.

(30) Korter, T. M.; Balu, R.; Campbell, M. B.; Beard, M. C.; Gregurick, S. K.; Heilweil, E. J. *Chem. Phys. Lett.* **2006**, *418*, 65–70.

(31) Kowalski, B. R.; Seasholtz, M. B. *J. Chemom.* **1991**, *5*, 219–145.

(32) (a) Legon, A. C.; Millen, D. J. *Chem. Rev.* **1986**, *86*, 635–657. (b) Legon, A. C.; Millen, D. J. *Acc. Chem. Res.* **1987**, *20*, 39–46.

(33) Diekmann, S. *EMBO J.* **1989**, *8*, 1–4.

(34) (a) Müller, A.; Talbot, F.; Leutwyler, S. *J. Chem. Phys.* **2000**, *112*, 3717–3725. (b) Müller, A.; Talbot, F.; Leutwyler, S. *J. Chem. Phys.* **2002**, *116*, 2836–2847. (c) Muller, A.; Talbot, F.; Leutwyler, S. *J. Am. Chem. Soc.* **2002**, *124*, 14486–14494. (d) Muller, A.; Talbot, F.; Leutwyler, S. *J. Chem. Phys.* **2001**, *115*, 5192–5202.

(35) (a) Held, A.; Pratt, D. W. *J. Am. Chem. Soc.* **1990**, *112*, 8629–8630. (b) Held, A.; Pratt, D. W. *J. Chem. Phys.* **1992**, *96*, 4869–4876.

JP8057614